Comparing GW+DMFT and LDA+DMFT for the testbed material $SrVO_3$

C. Taranto[1], M. Kaltak[2], N. Parragh[1,3], G. Sangiovanni[1,3], G. Kresse[2], A. Toschi[1], and K. Held[1]
[1] *Institute for Solid State Physics, Vienna University of Technology, 1040 Vienna, Austria*
[2] *University of Vienna, Faculty of Physics and Center for Computational Materials Science, Sensengasse 8/12, A-1090 Vienna, Austria and*
[3] *Institut für Theoretische Physik und Astrophysik, Universität Würzburg, Am Hubland, D-97074 Würzburg, Germany*
(Dated: Version 0, November 7, 2012)

We have implemented the GW+dynamical mean field theory (DMFT) approach in the Vienna ab initio simulation package. Employing the interaction values obtained from the locally unscreened random phase approximation (RPA), we compare GW+DMFT and LDA+DMFT against each other and against experiment for $SrVO_3$. We observed a partial compensation of stronger electronic correlations due to the reduced GW bandwidth and weaker correlations due to a larger screening of the RPA interaction, so that the obtained spectra are quite similar and well agree with experiment. Noteworthily, the GW+DMFT better reproduces the position of the lower Hubbard side band.

PACS numbers: 71.27.+a, 71.10.Fd

I. INTRODUCTION

The local density approximation (LDA) plus dynamical mean field theory (DMFT) approach[1–5] has been a significant step forward for calculating materials with strong electronic correlations. This is, because— on top of the LDA —DMFT[6,7] includes a major part of the electronic correlations: the local ones. In recent years, LDA+DMFT has been applied successfully to many materials and correlated electron phenomena, ranging from transition metals and their oxides to rare earth and their alloys, for reviews see Refs. 4,5.

For truly parameter-free *ab initio* calculations, however, two severe shortcomings persist: (i) the screened Coulomb interaction is usually considered to be an adjustable parameter in LDA+DMFT and (ii) the so-called double counting problem (i.e., it is difficult to determine the electronic correlations already accounted for at the LDA level). These shortcomings are intimately connected with the fact that the density functional nature of LDA does not match. with the many-body, Feynman-diagram structures of DMFT. Hence, it is not clear what correlations are already included on the LDA level or how to express these as a self-energy to avoid a double counting with DMFT correlations. These problems can be mitigated, but not solved, by constrained LDA (cLDA) calculations[8–10], which can be exploited to extract two independent parameters: interaction and double counting correction.[9,11]

A conceptionally preferable and better defined many-body approach is achieved if one substitutes LDA by the so-called GW approximation[12,13]. Since its proposition by Biermann *et al.*[14], the development and application of such a GW+DMFT scheme for actual applications has been tedious. This is reflected in the number of LDA+DMFT calculations for actual materials, which is of the order of a few hundred, compared to a single[15] GW+DMFT calculation for Ni[14], despite many advantages of GW+DMFT, such as the possible rigorous definition in terms of Feynman diagrams and the avoidance of introducing *ad hoc* parameters for the Coulomb interaction and double counting corrections. The reason for this imbalance is twofold. First, since the GW approach is computationally fairly demanding and complex, mature GW programs were missing in the past. Second, the GW+DMFT scheme is considerably more involved than LDA+DMFT, in particular, if calculations are done self-consistently and with a frequency dependent (screened) Coulomb interaction. Indeed, these concepts are presently tested on the model level[16,20]. Let us also note in this context that a frequency dependent interaction has been employed on top of an LDA bandstructure for $BaFe_2As_2$[17] and $SrVO_3$[18]

In this paper, we present results of our GW+DMFT implementation in the Vienna ab initio simulation package (VASP) for $SrVO_3$ and compare the GW+DMFT results to those of LDA+DMFT[21] as well as photoemission spectroscopy[22]. We find the GW+DMFT spectra to be quite similar to that of LDA+DMFT due to a partial cancellation of two effects: the reduced GW bandwidth in comparison to LDA and the weaker screened Coulomb interaction. An important difference, however, is the position of the lower Hubbard band which in GW+DMFT better agrees with experiment. To mimic the frequency dependence of the Coulomb interaction, which we have not included, we also performed GW+DMFT calculations for a Bose factor ansatz[19] reduced bandwidth. The obtained spectra are rather different from GW+DMFT without Bose factor and LDA+DMFT.

The paper is organized as follows: In Section II, we discuss the method and implementation. In Section III, we compare LDA+DMFT and GW+DMFT self energies and spectral functions. A comparison to photoemission experiments is provided in Section IV and a conclusion in Section V.

II. METHOD

Let us briefly outline the relevant methodological aspects. Starting point of our calculation is the *GW* implementation within (VASP).[30] Specifically, we first performed Kohn Sham density functional theory calculations using the local density approximation for $SrVO_3$ at the LDA lattice constant of $a = 3.78$ Å and determined the Kohn Sham one-electron orbitals $\phi_{n\mathbf{k}}$ and one-electron energies $\epsilon_{n\mathbf{k}}$. The position of the GW quasiparticle peaks were calculated by solving the linear equation

$$E^{QP}_{n\mathbf{k}} = \epsilon_{n\mathbf{k}} + Z_{n\mathbf{k}} \times Re[\langle\phi_{n\mathbf{k}}|T + V_{n-e} + V_H + \Sigma(\epsilon_{n\mathbf{k}})|\phi_{n\mathbf{k}}\rangle - \epsilon_{n\mathbf{k}}], \quad (1)$$

where T is the one-electron kinetic energy operator and V_{n-e} and V_H are the nuclear-electron potential and the Hartree-potential, respectively. Σ is the G_0W_0 self energy, and $Z_{n\mathbf{k}}$ is the renormalization factor evaluated at the Kohn-Sham eigenvalues.[29,30] The original Kohn Sham orbitals are maintained at this step. The Kohn Sham orbitals expressed in the projector augmented wave (PAW) basis are then projected onto maximally localized Wannier functions[33] using the Wannier90 code.[34] To construct an effective low-energy Hamiltonian for the t_{2g} vanadium orbitals, we follow Faleev, van Schilfgaarde and Kotani and approximate the frequency dependent G_0W_0 self-energy by an Hermitian operator $\bar{H}$ that reproduces the position of the quasiparticle peaks of the original self-energy exactly:[42,43]

$$\bar{H}_{mn,\mathbf{k}} = \frac{1}{2}[\langle\phi_{m\mathbf{k}}|\Sigma^*(E^{QP}_{m\mathbf{k}}) + \Sigma(E^{QP}_{n\mathbf{k}})|\phi_{n\mathbf{k}}\rangle]. \quad (2)$$

In practice, for the present calculations, we have applied the slightly more involved procedure to derive an Hermitian approximation outlined in Ref. 31, although this yields essentially an identical Hermitian operator $\bar{H}_{mn,\mathbf{k}}$. Furthermore the off diagonal components are found to be negligible small, and henceforth disregarded. The final Hermitian and **k**-point dependent operator $\bar{H}$ is transformed to the Wannier basis and passed on to the DMFT code, where it is used to construct the **k**-dependent self energy by adding the local DMFT self energy.

Fig. 1 shows the obtained G_0W_0 bandstructure, which for the t_{2g} vanadium target bands is about 0.7 eV narrower than for the LDA. The oxygen p band (below -2 eV) is shifted downwards by 0.5 eV compared to the LDA, whereas the vanadium e_g bands (located about 1.5 eV above the Fermi-level) are slightly shifted upwards by 0.2 eV. In the LDA, the top most vanadium t_{2g} band at the M point is slightly above the lowest e_g band at the Γ point, whereas the G_0W_0 correction opens a gap between the t_{2g} and e_g states.

For brevity we will refer to the subsequent DMFT calculations as GW+DMFT, although it should be kept in mind that no self-consistency is performed in the *GW* part and furthermore the *GW* self energy is approximated by an Hermitian (frequency in-dependent) non-diagonal operator. Subtracting the local part of this Hemritian operator (to avoid a double counting) yields for the degenerate t_{2g} orbitals a constant shift. This procedure allows to maintain the structure and outline of the common DFT-DMFT scheme and can be easily adopted in any DMFT code. However it neglects lifetime broadening introduced by other bands not treated on the DMFT level.

Within this Wannier basis, we also calculate the screened Coulomb interaction using the random phase approximation (RPA). As described in Ref. 35 for an accurate estimate of the interaction value to be used in DMFT (U^{DMFT}), only the local screening processes of the t_{2g} target bands of $SrVO_3$ are disregarded since only these are considered later on in DMFT. This approach[35] is similar to the constrained RPA (cRPA)[36,37], with the difference being that in cRPA also *non-local* screening processes of the t_{2g} target bands are disregarded which are not included in DMFT. We carefully compare *GW*+DMFT with LDA+DMFT calculations and experiment. In both cases we use (frequency-independent) interactions obtained from this locally unscreened RPA and cLDA. The Kanamori interaction parameters as derived from the locally unscreened RPA are: intra-orbital Coulomb repulsion $U^{\mathrm{DMFT}} = 3.44$ eV; inter-orbital Coulomb repulsion $\bar{U}^{\mathrm{DMFT}} = 2.49$ eV; Hund's exchange and pair hopping amplitude $J^{\mathrm{DMFT}} = 0.46$ eV.[46] These values are, for $SrVO_3$, almost identical to the cRPA.[35] In cLDA, on the other hand, somewhat larger interaction parameters were obtained and are employed by us for the corresponding calculations: $U^{\mathrm{cLDA}} = 5.05$ eV, $\bar{U}^{\mathrm{cLDA}} = 3.55$ eV, $J^{\mathrm{cLDA}} = 0.75$ eV.[22]

For the subsequent DMFT calculation, we employ the Würzburg-Wien w2dynamics code[39], based on the hybridization-expansion variant[40] of the continuous-time quantum Monte Carlo method (CT-QMC)[41]. This algorithm is particularly fast since it employs additional quantum numbers for a rotationally-invariant Kanamori interaction[39]. The maximum entropy method is employed for the analytical continuation of the imaginary time and (Matsubara) frequency CT-QMC data to real frequencies[47].

All our calculations are without self-consistency, which is to some extend justified for $SrVO_3$. Since the three t_{2g} bands of $SrVO_3$ are degenerate, DMFT does not change the charge density of the low-energy t_{2g} manifold and hence self-consistency effects are expected to be small for LDA+DMFT. This is, in principle, different for *GW*+DMFT. Here, the frequency dependence of the DMFT self energy might yield some feedback already for a simplified Faleev, van Schilfgaarde and Kotani quasiparticle self-consistency[42,43]. Finally, we also test the Bose factor ansatz[19] which renormalizes the *GW* bandwidth by a renormalization factor $\mathcal{Z}_B = 0.7$[19] for mimicking the frequency dependence of the (partially unscreened) RPA interaction.

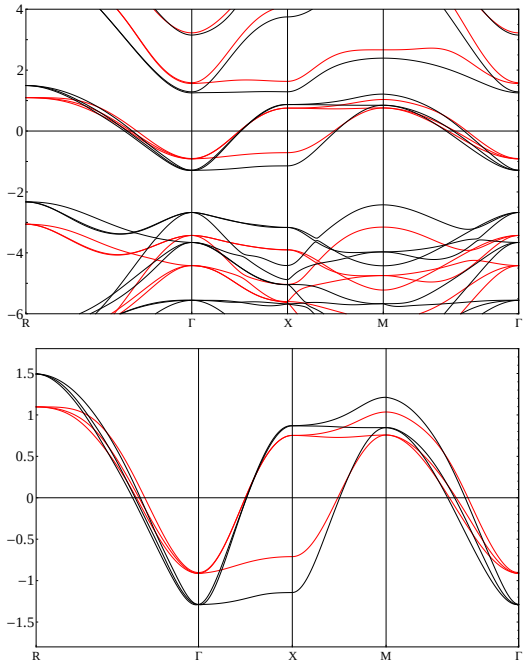

FIG. 1: (Color online) Upper panel: G_0W_0 quasiparticle bands (red, grey) in comparison to LDA (black). The Fermi level sets our zero of energy and is marked as a line. Lower panel: Wannier projected t_{2g} bandstructure from G_0W_0 (red, grey) and LDA (black). The t_{2g} target bands bandwidth is reduced by $\sim 0.7\,\mathrm{eV}$ in GW.

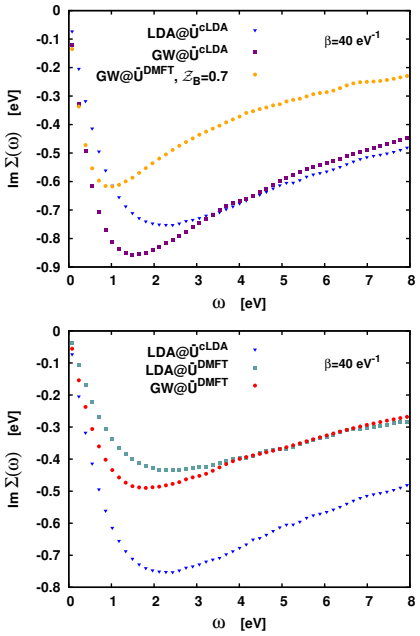

FIG. 2: (Color online) Comparison of the imaginary part of the DMFT self energies Σ vs. (Matsubara) frequency ω for $SrVO_3$ at inverse temperature $\beta = 40\ \mathrm{eV}^{-1}$ as computed in five different ways: employing GW and LDA Wannier bands, the locally unscreened RPA interaction $\bar{U}^{\mathrm{DMFT}} = 2.49$ eV and the cLDA $\bar{U}^{\mathrm{cLDA}} = 3.55\,\mathrm{eV}$, as well as the Bose factor renormalization of $\mathcal{Z}_B = 0.7$.[19]

III. RESULTS

For analyzing the differences between GW+DMFT and LDA+DMFT we analyze and compare in the following five different calculations:

1. LDA+DMFT@$\bar{U}^{\mathrm{cLDA}}$ (conventional LDA+DMFT calculation with the cLDA interaction $\bar{U}^{\mathrm{cLDA}} = 3.55\,\mathrm{eV}$).
2. LDA+DMFT@$\bar{U}^{\mathrm{DMFT}}$ (LDA+DMFT calculation but with the locally unscreened RPA interaction $\bar{U}^{\mathrm{DMFT}} = 2.49\,\mathrm{eV}$).
3. GW+DMFT@$\bar{U}^{\mathrm{DMFT}}$ (GW+DMFT calculation with $\bar{U}^{\mathrm{DMFT}} = 2.49\,\mathrm{eV}$)
4. GW+DMFT@$\bar{U}^{\mathrm{cLDA}}$ (GW+DMFT calculation but with $\bar{U}^{\mathrm{cLDA}} = 3.55\,\mathrm{eV}$)
5. GW+DMFT@$\bar{U}^{\mathrm{DMFT}}$,$\mathcal{Z}_B = 0.7$ (as 3. but with a Bose renormalization factor $\mathcal{Z}_B$)

Let us first turn to the imaginary part of the local self energy which is shown as a function of (Matsubara) frequency in Fig. 2. The self energy yields a first impression how strong the electronic correlations are in the various calculations. The LDA+DMFT@$\bar{U}^{\mathrm{DMFT}}$ self energy is the least correlated one, somewhat less correlated than LDA+DMFT@$\bar{U}^{\mathrm{cLDA}}$ due to the smaller locally unscreened Coulomb interaction ($\bar{U}^{\mathrm{DMFT}} = 2.49\,\mathrm{eV} < 3.55\,\mathrm{eV} = \bar{U}^{\mathrm{cLDA}}$). For the same reason also the GW+DMFT@$\bar{U}^{\mathrm{DMFT}}$ self energy is less correlated than that of a GW+DMFT@$\bar{U}^{\mathrm{cLDA}}$ calculation.

If we compare LDA+DMFT and GW+DMFT on the other hand, the LDA+DMFT self energy is less correlated than the GW+DMFT one, if the Coulomb interaction is kept the same. This is due to the 0.7 eV smaller GW t_{2g}-bandwidth in comparison to LDA. This observation also reflects in the DMFT quasiparticle renormalization factors Z which were obtained from a fourth-order fit to the lowest four Matsubara frequencies, see Table I. Note that there is an additional GW renormalization factor reducing the bandwidth in comparison to LDA.

However, the effect of the smaller GW bandwidth partially compensates with the smaller $\bar{U}^{\mathrm{DMFT}}$ interaction strength. Altogether this yields rather similar self energies of the standard approaches: LDA+DMFT@$\bar{U}^{\mathrm{cLDA}}$ and GW+DMFT@$\bar{U}^{\mathrm{DMFT}}$, see lower panel of Fig. 2. This also reflects in very similar renormalization factors in Table I, $Z = 0.51$ vs. $Z = 0.57$, which both agree well with experimental estimates of 0.5-0.6 .[22,45]

Since one important difference is the strength of the interaction, it is worthwhile recalling that $\bar{U}^{\mathrm{DMFT}}$ is defined as the local interaction strength at low frequencies. While this value is almost constant within the range of the t_{2g}-bandwidth, it is much larger at larger energies, exceeding 10 eV. It has been recently argued and shown in model calculations[19] that the stronger

Scheme	Z	$d_{\rm intra}$	$d^{\uparrow\uparrow}_{\rm inter}$	$d^{\uparrow\downarrow}_{\rm inter}$
LDA+DMFT@$\bar{U}^{\rm cLDA}$	0.51	0.004	0.013	0.009
LDA+DMFT@$\bar{U}^{\rm DMFT}$	0.67	0.007	0.016	0.013
GW+DMFT@$\bar{U}^{\rm DMFT}$	0.57	0.005	0.014	0.010
GW+DMFT@$\bar{U}^{\rm cLDA}$	0.39	0.003	0.010	0.007
GW+DMFT@$\bar{U}^{\rm DMFT}$,$\mathcal{Z}_B=0.7$	0.36	0.003	0.009	0.006
experiment[22,45]	∼0.5-0.6			

TABLE I: (Color online) DMFT quasiparticle renormalization factors Z from the five different calculations at inverse temperature $\beta = 40\,{\rm eV}^{-1}$. Also shown are the pairwise double occupations within the same orbital $d_{\rm intra}$ and between different orbitals with the same $d^{\uparrow\uparrow}_{\rm inter}$ and opposite spin $d^{\uparrow\downarrow}_{\rm inter}$. The "standard" LDA+DMFT@$\bar{U}^{\rm cLDA}$ and GW+DMFT@$\bar{U}^{\rm DMFT}$ calculations are similarly correlated and well agree with experiment. Using the cLDA interaction($\bar{U}^{\rm cLDA}$) for GW+DMFT or the locally unscreened RPA ($\bar{U}^{\rm DMFT}$) for LDA+DMFT yields a too strongly and too weakly correlated solution in comparison to experiment, respectively. Note that GW+DMFT becomes even more strongly correlated, if the Bose renormalization factor is included.

frequency-dependence of the screened Coulomb interaction at high energies is of relevance and can be mimicked by a Bose factor renormalization of the GW bandwidth. The latter has been determined as $\mathcal{Z}_B = 0.7$ for $SrVO_3$. We have tried to take this into account in the GW+DMFT@$\bar{U}^{\rm DMFT}$,$\mathcal{Z}_B = 0.7$ calculation. Due to the additional bandwidth renormalization, this calculation is very different from all others and yields the largest quasiparticle renormalization, i.e., $Z = 0.36$ is smallest.

Next, we compare the **k**-integrated spectrum in Fig. 3. At low-frequency we find the same trends as for the self-energy results: The "standard" GW+DMFT and LDA+DMFT at $\bar{U}^{\rm DMFT}$ and $\bar{U}^{\rm cLDA}$, respectively, yield a rather similar spectrum. In particular the quasiparticle peak has a similar weight and shape. However, a difference that we will come back to later on is found at larger frequencies: The GW+DMFT Hubbard bands are closer to the Fermi level in comparison to LDA+DMFT. If we perform GW+DMFT and LDA+DMFT at the "wrong" interaction strength (i.e., $\bar{U}^{\rm cLDA}$ and $\bar{U}^{\rm DMFT}$, respectively), we obtain a noticeable stronger and weaker correlated solution. This trend is also reflected in the double occupations presented in Table I. Finally, as in the case of the self-energy, the GW+DMFT@$\bar{U}^{\rm DMFT}$,$\mathcal{Z}_B = 0.7$ solution is much more strongly correlated, with Hubbard side bands at much lower energies.

IV. COMPARISON TO PHOTOEMISSION SPECTROSCOPY

An obvious question is whether LDA+DMFT or GW+DMFT yields "better" results. This question is difficult to answer and for the time being we resort to a comparison with experimental photoemission spectroscopy (PES)[22]. However, one should be well aware of the limitations of such a comparison. On the theory side, the involved approximations common to the calculations, as e.g. neglecting non-local correlations beyond the DMFT and GW level, or further effects, such as the electron-phonon coupling or the photoemission matrix elements, might bias the theoretical result in one way or the other. On the experimental side, care is in place, as well. The PES results considerably improved in the last years due to better photon sources. Furthermore, in Ref. 22 an oxygen p-background has been subtracted, which by construction removes all spectral weight below the region identified as the lower Hubbard band.

Fig. 4 compares the proposed LDA+DMFT and GW+DMFT (with and without Bose renormalization) with PES experiment. To this end, the theoretical results have been multiplied with the Fermi function at the experimental temperature of 20K and broadened by the experimental resolution of 0.1 eV. The height of the PES spectrum has been fixed so that its integral yields 1, i.e., accommodates 1 t_{2g}-electron, as in theory.

The GW+DMFT@$\bar{U}^{\rm DMFT}$ and LDA+DMFT@$\bar{U}^{\rm cLDA}$ have a quite similar quasiparticle peak, which also well agrees with experiment, as it was already indicated by the quasiparticle renormalization factor. A noteworthy difference is the position of the lower Hubbard band which is at $-2\,{\rm eV}$ for LDA+DMFT@$\bar{U}^{\rm cLDA}$ and $\sim -1.6\,{\rm eV}$ for GW+DMFT@$\bar{U}^{\rm DMFT}$. The latter is in agreement with experiment and a result of the reduced GW band width. Let us note that the sharpness and height of the lower Hubbard band very much depends on the maximum entropy method, which tends to overestimate the broadening of the high-energy spectral features. Hence, only the position and weight is a reliable result of the calculation.

As we have already seen, the Bose-factor renormalized GW+DMFT@$\bar{U}^{\rm DMFT}$,$\mathcal{Z}_B = 0.7$ calculation is distinct from both, GW+DMFT@$\bar{U}^{\rm DMFT}$ and LDA+DMFT@$\bar{U}^{\rm cLDA}$. It is also different from experiment with a much more narrow quasiparticle peak and a lower Hubbard band much closer to the Fermi level. A similar difference between static U on the one side and frequency dependent U was reported in Ref. 18. A difference of this magnitude is hence to be expected. In the course of finalizing this paper, we became aware of Ref. 44, in which Tomczak *et al.* report a GW+DMFT calculation with the full frequency dependence of the cRPA interaction for $SrVO_3$ obtaining good agreement with experiment as well.

V. CONCLUSION

We have carried out a careful comparison of LDA+DMFT, G_0W_0+DMFT and experiment for the case of $SrVO_3$, which is often considered to be a "benchmark" material for new methods. To this end, the LDA or G_0W_0 quasiparticle bandstructure was projected onto maximally localized Wannier orbitals for the t_{2g}

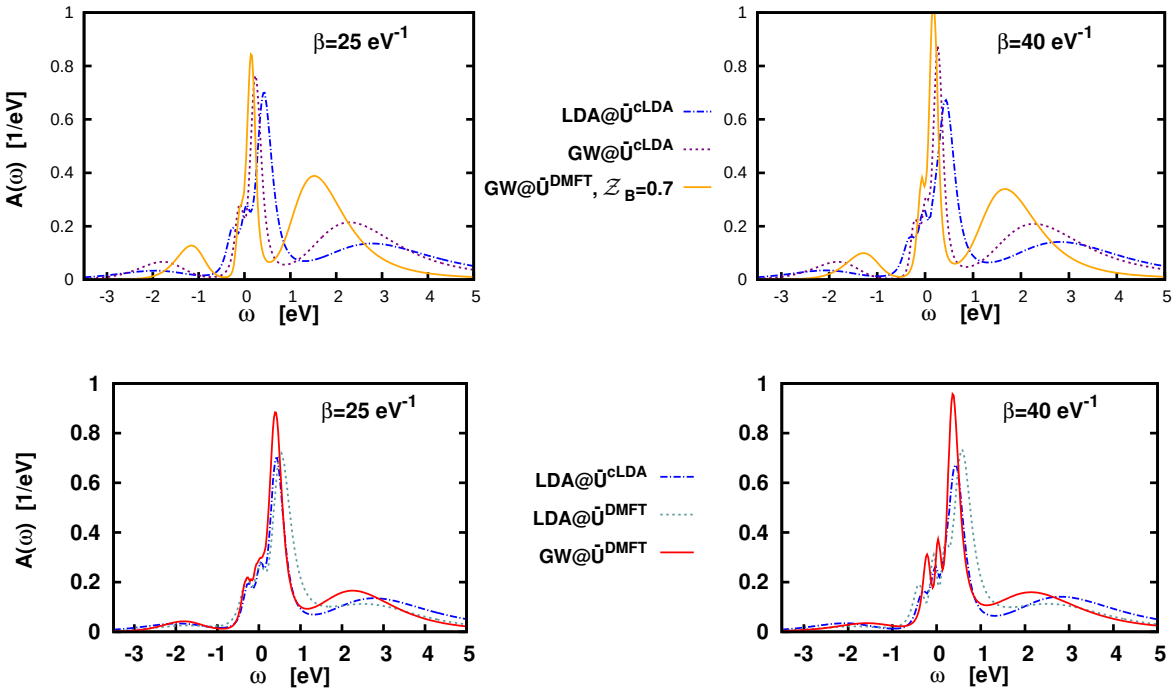

FIG. 3: (Color online) Spectral function for $SrVO_3$ computed in five different ways as in Fig. 2. At lower temperatures the central peak gets only slightly sharper and higher, although the temperature effects from $\beta = 25$ to $40\,\mathrm{eV}^{-1}$ are small.

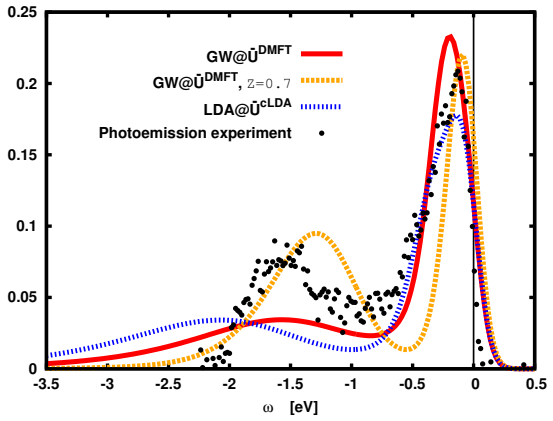

FIG. 4: (Color online) Comparison of LDA+DMFT@U^{cLDA}, GW+DMFT@U^{DMFT} (without and with Bose renormalization $\mathcal{Z}_B = 0.7$) and experiment. The position of the lower Hubbard band is better reproduced in GW+DMFT whereas the central peak is similar in LDA+DMFT and GW+DMFT. The Bose renormalization GW+DMFT differs considerably (photoemission spectra reproduced from Ref. 22).

bands. For these in turn correlation effects have been calculated on the DMFT level. If we take the locally unscreened RPA interaction (or the similar cRPA one) for the GW+DMFT and the cLDA interaction for LDA+DMFT, the two approaches yield rather similar self energies and spectral functions at the Fermi level. These also agree rather well with photoemission spectroscopy. A noteworthy difference between these two calculation is found, however, for the position of the lower Hubbard band, which is better reproduced in GW+DMFT. Similar spectra were also obtained by Tomczak *et al.*[44] using a GW+DMFT calculation including the frequency dependence of the interaction.

We thank R. Arita, S. Biermann, K. Nakamura, Y. Nomura, M. Imada, S. Sakai, and J. Tomzcak for many helful discussions. We acknowledge financial support from Austrian Science Fund (FWF) through project ID I597 (as part of the DFG Research Unit FOR 1346) and the SFB ViCom F4103. Calculations have been done on the Vienna Scientific Cluster (VSC).

[1] V. I. Anisimov, A. I. Poteryaev, M. A. Korotin, A. O. Anokhin and G. Kotliar, J. Phys. Cond. Matter **9** 7359 (1997).
[2] A. I. Lichtenstein and M. I. Katsnelson, Phys. Rev. B **57** 6884 (1998).
[3] K. Held, I. A. Nekrasov, G. Keller, V. Eyert, N. Blümer, A. K. McMahan, R. T. Scalettar, T. Pruschke, V. I. Anisimov, and D. Vollhardt, Psi-k Newsletter **56**, 5 (2003) and phys.

stat. sol. B **243**, 2599 (2006).
[4] G. Kotliar, S. Y. Savrasov, K. Haule, V. S. Oudovenko, O. Parcollet, C. A. Marianetti, Rev. Mod. Phys. **78**, 865 (2006).
[5] K. Held, Adv. Phys. **56** , 829 (2007).
[6] W. Metzner and D. Vollhardt, Phys. Rev. Lett. **62**, 324 (1989); A. Georges and G. Kotliar, Phys. Rev. B **45**, 6479 (1992).
[7] A. Georges, G. Kotliar, W. Krauth, and M. Rozenberg, Rev. Mod. Phys. **68**, 13 (1996).
[8] P. H. Dederichs, S. Blügel, R. Zeller and H. Akai, Phys. Rev. Lett. **53** 2512 (1984).
[9] A. K. McMahan, R. M. Martin and S. Satpathy, Phys. Rev. B **38** 6650 (1988).
[10] O. Gunnarsson, O. K. Andersen, O. Jepsen and J. Zaanen, Phys. Rev. B **39** 1708 (1989).
[11] For an example where U and the double counting correction have actually been obtaioned independently see A. K. McMahan, C. Huscroft, R. T. Scalettar and E. L. Pollock, J. Comput.-Aided Mater. Design **5** 131 (1998).
[12] L. Hedin, Phys. Rev. A **139** 796 (1965).
[13] F. Aryasetiawan and O. Gunnarsson, Rep. Prog. Phys. **61** 237 (1998).
[14] S. Biermann, F. Aryasetiawan, and A. Georges, Phys. Rev. Lett. **90** 086402 (2003).
[15] In the course of finalizing this paper, we became aware of a second GW+DMFT calculation: in a most recent preprint[44] Tomczak *et al.* studied, independently of us, $SrVO_3$ as well.
[16] P. Sun, G. Kotliar, Phys. Rev. B **66**, 85120 (2002).
[17] P. Werner, M. Casula, T. Miyake, F. Aryasetiawan, A.J. Millis, and S. Biermann, Nat. Phys. **8**, 331 (2012).
[18] M. Casula, A. Rubtsov, and S. Biermann, Phys. Rev. B **85**, 035115 (2012).
[19] M. Casula, P. Werner, L. Vaugier, F. Aryasetiawan, T. Miyake, A. J. Millis, and S. Biermann, Phys. Rev . Lett. **109**, 126408 (2012).
[20] T. Aryal, P. Werner, and S. Biermann, arXiv:1205.5553; arXiv:1210.2712.
[21] Let us note that $SrVO_3$ is the material arguably most well investigated by LDA+DMFT. Previous LDA+DMFT calculations include 22–26, cf. 18.
[22] A. Sekiyama, H. Fujiwara, S. Imada, S. Suga, H. Eisaki, S. I. Uchida, K. Takegahara, H. Harima, Y. Saitoh, I. A. Nekrasov, G. Keller, D. E. Kondakov, A. V. Kozhevnikov, Th. Pruschke, K. Held, D. Vollhardt and V. I. Anisimov, Phys. Rev. Lett. **93** 156402 (2004).
[23] E. Pavarini, S. Biermann, A. Poteryaev, A. I. Lichtenstein, A. Georges and O. K. Andersen, Phys. Rev. Lett. **92** 176403 (2004).
[24] A. Liebsch, Phys. Rev. Lett. **90** 096401 (2003).
[25] I. A. Nekrasov, G. Keller, D. E. Kondakov, A. V. Kozhevnikov, T. Pruschke, K. Held, D. Vollhardt and V. I. Anisimov, Phys. Rev. B **72** 155106 (2005).
[26] I. A. Nekrasov, K. Held, G. Keller, D. E. Kondakov, T. Pruschke, M. Kollar, O. K. Andersen, V. I. Anisimov and D. Vollhardt, Phys. Rev. B **73** 155112 (2006).
[27] K. Byczuk, M. Kollar, K. Held, Y.-F. Yang, I. A. Nekrasov, T. Pruschke and D. Vollhardt , Nature Physics **3** 168 (2007).
[28] S. Aizaki, T. Yoshida1 K. Yoshimatsu, M. Takizawa, M. Minohara, S. Ideta, A. Fujimori, K. Gupta, P. Mahadevan, K. Horiba, H. Kumigashira, and M. Oshima Phys. Rev. Lett. **109**, 056401 (2012).
[29] M. S. Hybertsen and S. G. Louie, Phys. Rev. B **34**, 5390 (1986).
[30] M. Shishkin and G. Kresse, Phys. Rev. B **74**, 035101 (2006).
[31] M. Shishkin, M. Marsman, and G. Kresse, Phys. Rev. Lett. **99**, 246403 (2007).
[32] C. Franchini, R. Kovacik, M. Marsman, S. Sathyanarayana Murthy, J. He, C. Ederer, and G. Kresse, J. Phys.: Condens. Matter **24**, 235602 (2012).
[33] N. Marzari and D. Vanderbilt, Phys. Rev. B **56** 12847 (1997).
[34] A. A. Mostofi, J. R. Yates, Y.-S. Lee, I. Souza, D. Vanderbilt and N. Marzari, Comput. Phys. Commun. **178**, 685 (2008).
[35] Y. Nomura, M. Kaltak, K. Nakamura, C. Taranto, S. Sakai, A. Toschi, R. Arita, K. Held, G. Kresse, and M. Imada, Phys. Rev. B **86**, 085117 (2012).
[36] F. Aryasetiawan, M. Imada, A. Georges, G, Kotliar, S. Biermann and A. I. Lichtenstein, Phys. Rev. B **70**, 195104 (2004).
[37] T. Miyake, F. Aryasetiawan, M. Imada, arXiv:0906.1344.
[38] F. Aryasetiawan, S. Biermann and A. Georges, In *Proceedings of the conference on "Coincidence Studies of Surfaces, Thin Films and Nanostructures"*, edited by A. Gonis (Wiley, New York, 2004). 4-4.
[39] N. Parragh, A. Toschi, K. Held, and G. Sangiovanni, arXiv:1209.0915 (accepted for publication in Phys. Rev. B).
[40] P. Werner, A. Comanac, L. De Medici, M. Troyer and A. J. Millis, Phys. Rev. Lett. **97** 076405 (2006).
[41] A. N. Rubtsov and A. I. Lichtenstein, JETP Lett. **80** 61 (2004).
[42] S. V. Faleev, M. van Schilfgaarde, and T. Kotani, Phys. Rev. Lett. **93**, 126406 (2004).
[43] A. N. Chantis, M. van Schilfgaarde, and T. Kotani, Phys. Rev. Lett. **96**, 086405 (2006).
[44] J. M. Tomczak, M. Casula, T. Miyake, F. Aryasetiawan, and S. Biermann, arXiv:1210.6580.
[45] K, Maiti, U. Manju, Sugata Ray, Priya Mahadevan, I. H. Inoue, C. Carbone, and D. D. Sarma, Phys. Rev. B **73**, 052508 (2006). M. Takizawa, M. Minohara, H. Kumigashira, D. Toyota, M. Oshima, H. Wadati, T. Yoshida, A. Fujimori, M. Lippmaa, M. Kawasaki, H. Koinuma, G. Sordi, and M. Rozenberg, Phys. Rev. B **80**, 235104 (2009)
[46] Note that the values differ slightly from the VASP values publsihed in Ref. 35 since with additional data, we have further improved the extrapolation.
[47] M. Jarrell and J. E. Gubernatis, Physics Reports **269** 133 (1996).
[48] Note that due to the presence of kinks there are actually two such renormalization factors[25,27,28]: a Fermi liquid $Z_{\rm FL}$ for the renormalization at the lowest energies and a second $Z_{\rm CP}$ for higher energies. The latter also corresponds to the overall weight of the central peak. With the energy resolution in Fig. 2 being limited by the discrete Matsubara frequencies the Z of Table I still rather corresponds to $Z_{\rm CP}$ as do the experimental valuies of 22,45.